

Detection of Fecal Contamination on Cantaloupes Using Hyperspectral Fluorescence Imagery

ANGELA M. VARGAS, MOON S. KIM, YANG TAO, ALAN M. LEFCOURT,
YUD-REN CHEN, YAGUANG LUO, AND YOONSEOK SONG, AND ROBERT BUCHANAN

ABSTRACT: To determine whether detection of fecal contamination on cantaloupes is possible using fluorescence imaging, hyperspectral images of cantaloupes artificially contaminated with a range of diluted bovine feces were acquired from 425 to 774 nm in responses to ultraviolet-A (320 to 400 nm) excitation. Evaluation of images at emission peak wavelengths indicated that 675 nm exhibited the greatest contrast between feces contaminated and untreated surface areas. Two-band ratios compared with the single-band images enhanced the contrast between the feces contaminated spots and untreated cantaloupe surfaces. The 595/655-nm, 655/520-nm, and 555/655-nm ratio images provided relatively high detection rates ranging from 79% to 96% across all feces dilutions. However, both single band and ratio methods showed a number of false positives caused by such features as scarred tissues on cantaloupes. Principal component analysis (PCA) was performed using the entire hyperspectral images data; 2nd and 5th principal component (PC) image exhibited differential responses between feces spots and false positives. The combined use of the 2 PC images demonstrated the detection of feces spots (for example, minimum level of 16- $\mu\text{g}/\text{mL}$ dry fecal matter) with minimal false positives. Based on the PC weighing coefficients, the dominant wavelengths were 465, 487, 531, 607, 643, and 688 nm. This research demonstrated the potential of multispectral-based fluorescence imaging for online applications for detection of fecal contamination on cantaloupes.

Keywords: hyperspectral imaging, fluorescence, cantaloupe, fecal contamination, ratio image

Introduction

Spurred by multiple outbreaks of foodborne illness associated with fresh produce and the identification of fecal contamination as the major source of pathogens responsible for these outbreaks, the United States Dept. of Agriculture (USDA) has instituted a number of programs to attempt to reduce fecal contamination of food products. In addition, the Food and Drug Administration issued the *Guide to Minimize Microbial Food Safety Hazards for Fresh Fruits and Vegetables* (USFDA 1998). Fruits and vegetables can become contaminated with pathogens through contact with soil, animals, or humans during any stage of the food-handling chain, including growing and harvesting operations as well as while in the processing plants (Murdock and Brokaw 1957). In general, foodborne pathogens originate from the intestinal tracts of animals and humans (USFDA 2001), thus making fecal matter a major source of contamination. For example, fecal contamination can result from use of manure-based fertilizers, and unsanitary conditions in processing and packaging plants.

Outbreaks of salmonellosis have been epidemiologically linked to consumption of fresh cantaloupes (USFDA 2001); as a consequence, this produce has been targeted as a potentially hazardous food. Contaminated cantaloupes were found to be responsible for 2 deaths and 18 hospitalizations due to *Salmonella* between 2000

and 2002; subsequent investigations revealed unsanitary growing and packaging conditions (Anderson and others 2002; USFDA 2002). USFDA investigations noted a broad range of potential factors, such as field irrigation with sewage-contaminated water, poor hygienic practices of workers, pests in packing facilities, and inadequate cleaning and sanitizing of equipment (USFDA 2001).

The Instrumentation and Sensing Laboratory of the USDA in Beltsville, Md., has developed a hyperspectral imaging system (HIS). The system provides a noninvasive method to assess hazardous conditions for fresh produce, is capable of acquiring reflectance and fluorescence measurements, and has been successfully used to demonstrate the detection of fecal contamination on apples and other fresh produce (Kim and others 2001). Hyperspectral imaging systems can simultaneously collect spectral data for hundreds of narrow contiguous wavebands over regions of the electromagnetic spectrum at every spatial pixel in an image. The resulting spectra can serve as fingerprints or signatures for target identification. For food safety applications, a central goal of using hyperspectral imaging data is to find several spectral bands that can be implemented to the development of multispectral inspection systems for online applications at processing plants (Chen and others 2002).

Many image-processing techniques have been developed to identify targets, increase image interpretation reliability, and improve classification. Image fusion is one such technique, defined by Van Genderen and Pohl (1994) as "the combination of 2 or more images to form a new image by using a certain algorithm." Applicable to various types of data sets, its main purposes for digital imagery are to sharpen images, improve geometric correlation, and enhance certain features not readily apparent in single images. Image fusion includes mathematical combinations of spectral images in arithmetic operations and techniques such as principal component analysis (PCA).

MS20050015 Submitted 1/7/05, Revised 3/2/05, Accepted 6/15/05. Authors Vargas and Tao are with Biological Resources Engineering, Univ. of Maryland, College Park, Md. Authors Kim, Lefcourt, and Chen are with USDA-ARS, Instrumentation and Sensing Laboratory, Beltsville, MD 20705. Author Luo is with USDA-ARS, Food Quality and Safety Laboratory, Beltsville, Md. Author Song is with FDA/NCFST, Div. of Food Processing and Packaging, Summit-Argo, Ill. Author Buchanan is with FDA/CFSAN, College Park, Md. Direct inquiries to author Kim (E-mail: kimm@ba.ars.usda.gov).

For this investigation, hyperspectral fluorescence images were collected from cantaloupes artificially contaminated with bovine feces at varying concentrations. The objective of the present study was to identify a few wavelength bands that could be used to detect fecal contamination on cantaloupes. To enhance the detection process, the selected wavelength bands were subjected to 2-band ratio permutations and an unsupervised classification method was used on the resultant images. In addition, the entire hyperspectral images were subjected to PCA, and principal component (PC) images were evaluated for fecal contamination detection and determination of multispectral bands.

Materials and Methods

Sample preparation

Forty Western Shipper cantaloupes were purchased from a local supermarket. To increase the number of samples and prevent sample movement during HIS scanning, cantaloupes were cut in half, and the 80 halves placed cut-side down in batches of 8 on black trays. Hyperspectral images were 1st collected for all 80 samples before any treatment. Fresh feces from the USDA dairy farm in Beltsville, Md. were diluted by weight to 1:10, 1:50, 1:100, 1:300, and 1:500 with deionized water. Dry fecal matter concentration for 1:100 dilution was 16 $\mu\text{g}/\text{mL}$ as determined by drying samples to constant weight in a 90 °C oven. Using a variable pipette, a matrix of dilutions was applied to each sample at 40, 30, 20, and 10 μL (Figure 1). Samples were allowed to air-dry with the aid of a fan for several hours until fecal spots were completely dried, and then scanned again. It was observed that areas contaminated with the 1:10 dilution were usually visible to the human eye. As dilutions increased, spots became transparent and less visible. At 1:100 dilutions, contaminated spots became difficult to visually identify. Digital color photos of samples were acquired prior to taking hyperspectral images.

Hyperspectral fluorescence images acquisition

A hyperspectral imaging system incorporating a line scan spectrograph with a spectral resolution of approximately 7-nm full width at half maximum (FWHM) was used to acquire images (Kim and others 2001). A motorized table was used to move samples at 1-mm intervals, and the zoom lens was adjusted to yield a pixel resolution of 1 mm^2 . The effective spectral range for fluorescence imaging was from 425 nm to 774 nm, with about 4.5-nm intervals, which was captured using 79 spectral channels. Two continuous wave UV-A (360 nm)

fluorescent lamp assemblies provided the samples with a near-uniform illumination. The system was operated under dark conditions. A more detailed description of the system operation is given by Kim and others (2004), and calibration is given by Kim and others (2001). Each batch of 8 cantaloupes required approximately 5 min to scan. The line scan data was saved in 16-bit binary files and processed later to create hyperspectral image cubes containing spatial and spectral data. Software developed in Visual Basic version 6 (Microsoft, Seattle, Wash., U.S.A.) was used to acquire data and to perform further processing. Additional data analyses were done using ENVI version 3.2 (Research System Inc., Boulder, Colo., U.S.A.).

Data processing and analyses

The spectral dimension was smoothened using a 3-point running average before image visualization or analyses. Masks to eliminate background were created manually using threshold values determined by evaluating background pixel intensities. The largest possible rectangular region of interest (ROI) within each fecal spot was used to extract representative spectral data. Images taken before treating the samples were used to create spectra of uncontaminated surfaces. ROI for untreated cantaloupes encompassed the largest rectangular area within the sample. The averaged ROI fluorescence spectra were used to characterize fluorescence emission of feces and untreated cantaloupe surfaces. Images at individual wavebands where spectra showed emission peaks were visually evaluated for efficacy of fecal contamination detection. Fecal spots for all dilutions and volumes were visually tallied from the selected single-band images.

All possible ratio permutations of emission peak and valley wavelengths were generated. These ratio images were visually assessed for fecal contamination detection and the best ratio images were selected. Subsequently, selected ratio images were subjected to an unsupervised classification method, ISODATA (Iterative Self-Organizing Data Analysis Technique), which clusters pixels into a desired number of classes without any a priori information about the classes (Ball and Hall 1965). Pixels with similar intensities are grouped into distinct classes by calculating class means evenly distributed in the data space; the remaining pixels are then iteratively clustered using minimum distance techniques until the number of pixels in each class change by less than the selected pixels change threshold. The sum of the square error (SSE), commonly used as clustering principle, is expressed as:

$$SSE = \sum_{C_i} \sum_{x \in C_i} (x - m_i)^2 = \sum_{C_i} \sum_{x \in C_i} \|x - m_i\|^2$$

where m_i is the mean of the i th cluster, $x \in C_i$ is a pattern assigned to that cluster and the outer sum, and \sum_{C_i} is the sum over all the clusters (Richards 1986). Only 1 iteration was used to recalculate means, and the threshold parameter was set at 5%. The number of classes was selected based on the number of possible features found on the surface of cantaloupes, such as rind and vein tracts, bruises, cuts, variations in coloration, and fecal spots. For this study, classes ranged between 5 and 10, with no less than 3 pixels per class. Subsequently, several classes in the resulting images were merged to produce a binary image of feces contaminated regions and background.

In addition, the entire image data set (79 channels) was subjected to PCA. In the process of creating the PCA images, a correlation matrix of the image is calculated. This correlation matrix is a diagonal matrix, which is then used to compute the eigenvalues. The eigenvalues are equivalent to the variance of each PC image. The

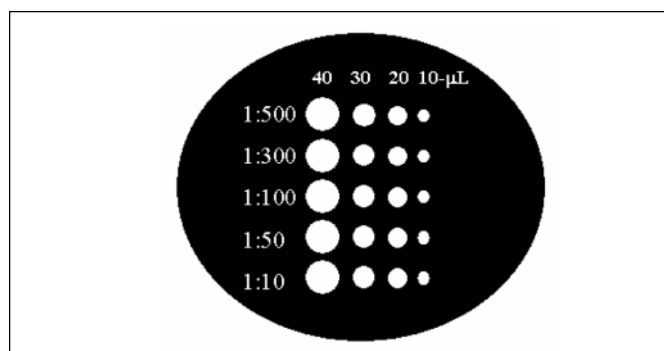


Figure 1—Schematic illustration of sample treatments. Using a variable pipette, bovine feces at 1:500, 1:300, 1:100, 1:50, and 1:10 dilutions were applied to the cantaloupe halves in volumes of 10, 20, 30, and 40 μL . Fecal matter content for 1:100 dilution was 16 $\mu\text{g}/\text{mL}$ as determined by drying sample to constant weight in a 90 °C oven.

resulting matrix A is diagonalized by an orthogonal eigenvectors matrix (E), and D is a diagonal matrix (Lay 2002).

$$A = EDE^t$$

As explained by Pohl and Van Genderen (1998), PCA transforms the original data set into a set of new uncorrelated linear combinations of the original variables. In this manner, PCA restructures the data so that most of the variance in the original data is accounted for in a reduced number of variables. The images are then ordered in terms of variance sizes, where the 1st PC accounts for the largest variance.

Results and Discussion

Spectral responses

Figure 2 shows the averaged fluorescence spectra for areas treated with 40 μ L of fecal contamination at 1:10, 1:50, 1:100, and 1:300 dilutions, and for untreated sample areas. For the feces treated spots, the average size of the rectangular ROI was 52 pixels (with a minimum of 20 and maximum of 99). For untreated spots, the average size of the rectangular ROI was 13845 pixels (with a minimum of 11880 and maximum of 15720). Fecal spots for 1:500 dilutions were difficult to identify, suggesting that they were similar to uncontaminated areas. For this reason, the averaged spectrum for dilutions of 1:500 was not shown in (Figure 2).

The spectra show fluorescence emission peaks in the green region at 520, 555, and 595 nm, and an additional peak for the feces treated spots in the red at 675 nm. At high feces concentrations, 1:10 and 1:50 dilution spots, there was a distinct response in the green region due to the presence of feces in that relative fluorescence intensities were lower compared with the 1:100, 1:300, and 1:500 dilution spots. This observation was the results of reabsorption characteristics of animal fecal matter existing in relatively high concentrations (Kim and others 2004). The application of the 1:100 and 1:300 dilutions resulted in transparent feces spots, and the fluorescence responses in the green bands resembled those of untreated areas.

Fluorescence emissions in the 650 to 750 nm region from intact green plant materials are due to membrane-bound chlorophyll a with emission maxima at 685 nm and 730 nm (Papageorgiou 1975). The averaged spectrum for untreated cantaloupe surfaces exhibited very low chlorophyll a fluorescence emission, indicating a well-ripened state of the samples. However, animal fecal matter showed blue-shifted emission peak at 675 nm, which emanated from chloro-

phyll a and its by-products such as pheophorbide a (Kim and others 2003). Multiple plant constituents, including phenolic compounds and riboflavin, are responsible for the fluorescence emission in the blue-green region of the spectrum (Chappelle and others 1991; Kim and others 2001). Other factors that may affect fluorescence emissions include changes in accumulation of the anthocyanin pigments in association with fruit ripeness (Abbott and others 1997).

Figure 3 shows representative gray-scale fluorescence images of cantaloupes contaminated with feces at 520, 555, 595, and 675 nm. These wavelengths correspond to fluorescence emission maxima observed in the representative fluorescence spectra (Figure 2). In general, the images illustrated progressive decreases in intensities from the center portions toward the edges due to the hemispherical shapes of the cantaloupe halves. In addition, intensity variations in localized regions (asides from the feces treated spots) were noted, suggesting heterogeneous nature of the cantaloupe surfaces in fluorescence responses. In the green region bands at 520, 555, and 595 nm, 1:10 and 1:50 dilution spots were shown darker than surrounding cantaloupe surfaces. For 1:300 and 1:500 dilution spots, the visual identification was difficult; as these dilutions created transparent feces contaminated spots, the fluorescence responses started to blend with those of cantaloupe surfaces. Fluorescence responses at 675 nm were markedly different than those of the green bands in that feces contaminated spots were brighter than cantaloupe surfaces. Similar responses were observed on apples contaminated with bovine feces and this observation was attributed to additive effects of fluorescent animal feces and apples (Kim and others 2003).

Detection results based on the visual assessment of the 520-nm, 555-nm, 595-nm, and 675-nm bands for 40- μ L spots are shown in Figure 4. Results for other feces volumes were similar and omitted for brevity. All the wavelength images showed evidence (95% to 100% detection rates) of the 1:10 feces dilution spots. The 675-nm band demonstrated the best potential for detection of feces across the range of volumes and concentrations tested (95% to 73% detec-

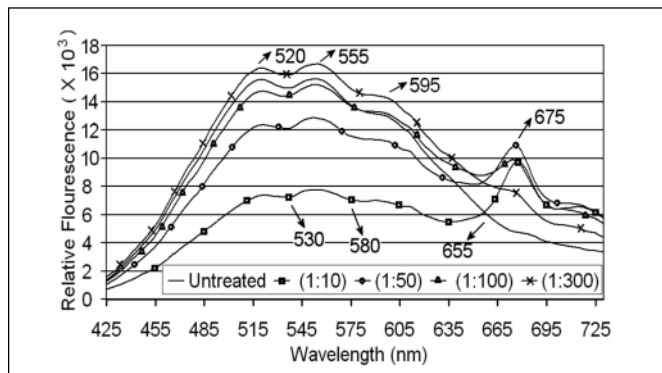


Figure 2—Representative fluorescence spectra obtained from the region of interests (ROI). Note that spectrum for 1:500 dilution spot was not included because the spectral characteristics were similar to those of the cantaloupe surfaces.

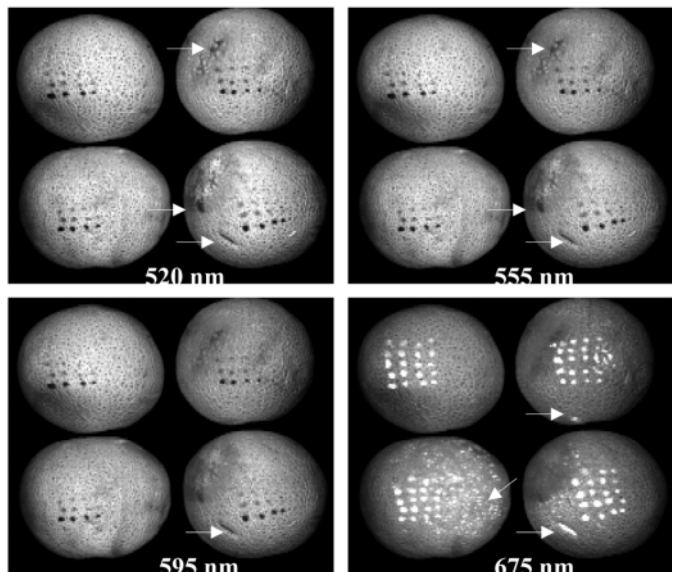


Figure 3—Fluorescence images of bovine-feces treated cantaloupes acquired using the Instrumentation and Sensing Laboratory (ISL) hyperspectral imaging system. The wavelengths correspond to fluorescence emission maxima observed in the representative spectra. Arrows indicate some potential false positives in the images. Cantaloupe in the bottom right corner shows a physical damage (scarred tissues).

tion rates for 1:10 to 1:500 dilution spots, respectively); although 100% of the 1:10 dilution spots could be detected at the green bands, detection rates for 1:300 and 1:500 dilutions were zero. Based on the single-band imaging, most of the cantaloupes exhibited a number of false positives (Figure 3), which could be attributed to physical damage such as bruises or cuts (scarred tissues). False positives in the red (650 to 700 nm) region of the spectrum may also emanate from netted rind and vein tracts that contained chlorophyll *a*. For the green band images, the relatively lower fluorescence intensities of the edge portions of cantaloupes were also potential false positives.

Ratio images

Although single-waveband images showed potential for detection of fecal matters on cantaloupes, mathematical combinations of images acquired at different wavelengths can enhance fecal contamination detection and reduce false positives. Addition and multiplication of images have been shown to enhance contrast, whereas difference or ratio images are suitable for detecting changes (Pohl and Van Genderen 1998). Kim and others (2002) effectively demonstrated the use of ratio methods to isolated fecal contaminated spots from apples of different varieties. For this investigation, the most promising results were also obtained with 2-band ratio images. Thus, discussion is limited to those ratios that resulted in high detection rates for brevity.

Representative gray-scale, 2-band ratio images (595/655, 655/520, and 555/655 nm), and ratio images subjected to the ISODATA method are shown in Figure 5a and 5b, respectively. These ratios compared with the single-band images enhanced the contrast between the feces treated spots and cantaloupe surfaces and produced more uniform responses across the cantaloupe surfaces. Detection results for 40- μ L spots ($n = 80$ per dilution) for 595/655-nm, 655/520-nm, 555/655-nm, and 675/555-nm ratio images are shown in Figure 6. The 595/655-nm ratio image followed by 655/520 nm, 555/655 nm, and 675/555 nm achieved relatively high detection rates across all feces concentrations. Note that ratio images shown in Figure 5 excluded the use of the best single band at 675 nm in the ratio combinations.

For reducing false positives, the 595/655-nm and 555/655-nm ratio images provided the most satisfactory results (Figure 5b) with detection rates ranging 80% to 95% and 79% to 91%, respectively, for 1:500 to 1:10 feces dilution spots. With the use of the ISODATA method, removal of clusters of 3 pixels or less resulted in the exclusions of some false positives. However, false positives were still

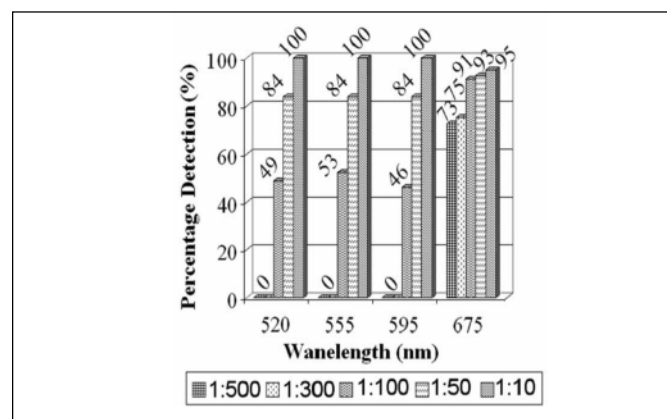


Figure 4—Fecal-contamination detection rates for 40- μ L treatment spots based on the single-wavelength images at 520 nm, 555 nm, 595 nm, and 675 nm ($n = 80$ per dilution)

apparent; the most prominent false positives were due to the scarred tissues as indicated on the lower-right cantaloupe in Figure 5.

Principal component analysis

Figure 7 illustrates representative 1st PC (PC-1) to 6th PC (PC-6) images obtained from the PCA of the entire hyperspectral fluorescence image data. PC-1 through PC-6 accounted for 99.94% of the data variability and images beyond PC-6 contained no useful attributes for detection of feces treated spots. The PC-1 image reflects a weighted sum of all the spectral bands and showed features causing the largest variations of the data; the intensity decreases from the center portions to the edges of the cantaloupe surfaces. Subsequent PC images depicted other features affecting variations in spectral responses. For instance, PC-3, PC-4, and PC-6 images showed responses that may be attributes of color variations or sides in contact with the grounds (ground spots).

PC-2 and PC-5 images exhibited the evidence of the feces-treated spots as darker and lighter spots, respectively, in contrast to the cantaloupe surfaces. In addition, PC-5 showed the scarred tissues (on the lower-right cantaloupe) that were false positives in the single-band and ratio images as non-false positives. PC-2 and PC-5 images were subjected to a simple thresholding method (Kim and others 2004) to create binary images for fecal contamination spots (Figure 8a and 8b). These images exhibited false positives. However, the PC-

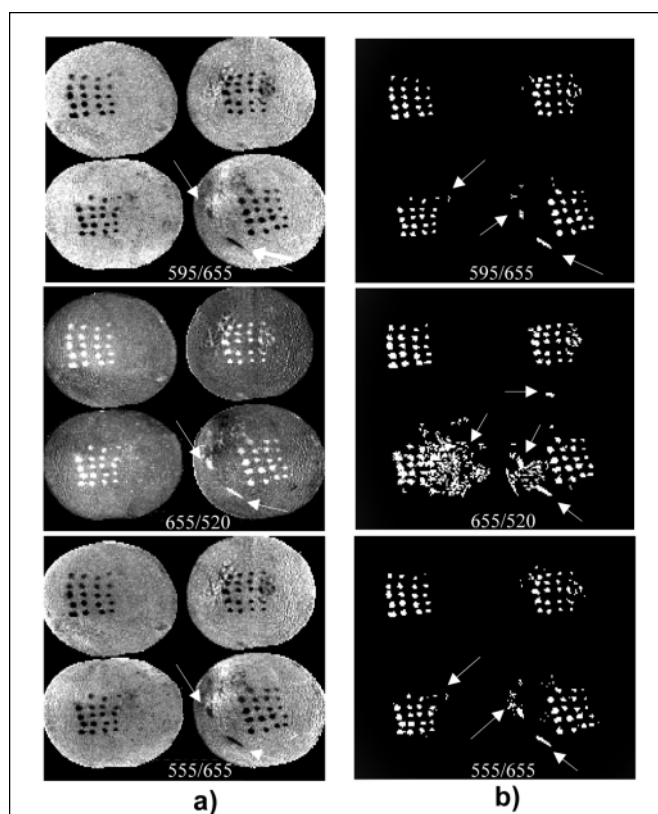


Figure 5—(a) Representative 2-band ratio images of 595/655, 655/520, and 555/655 nm. Out of all possible 2-band ratio permutations of peak and valley wavelengths observed in the fluorescence spectra, these ratios provided the best contrast between the feces-treated spots and cantaloupe surfaces and produced more uniform responses across the cantaloupe surfaces. (b) Binary images for feces-contamination spots obtained by subjecting ratio images to the ISODATA method. Arrows indicate some false positives. 595/655-nm and 555/655-nm ratios were the most effective in reducing false positives.

2 false positives did not coincide with those of PC-5. Figure 8c shows the spots (pixels) where the PC-2 and PC-5 binary images overlapped. Although the combined use of PC-2 and PC-5 compromised the detection of some 1:300 and 1:500 spots, the resultant image in Figure 8c illustrated the 1:10, 1:50, and 1:100 spots (a minimum of 16- μ g/mL dry fecal matter) with minimal false positives.

The PCA was performed using the data in entire spectral regions. However, individual PC images could be approximated by the use of

few significant wavelengths (Kim and others 2002). Figure 9 shows weighing coefficients (eigenvectors) for the PC-2 and PC-5 images. The peaks and valleys indicated the dominant wavelengths, 487 and 607 nm for PC-2, and 465, 531, 643, and 688 nm for PC-5. Weighted sums of the original images at the dominant wavelengths can create near-identical images comparable to the PC-2 and PC-5 images, respectively. Above wavelengths can be implemented to a multispectral imaging system for online applications. Readily available common aperture-based, multispectral adaptors can be used to simultaneously capture images up to 8 spectral bands (Chen and other 2002). Further research is needed to incorporate samples with various stages of maturity and to develop automated processing and detection methods for online applications.

Conclusions

In this investigation, hyperspectral fluorescence images were evaluated for detection of fecal contamination on cantaloupes. Single waveband images showed natural variations in fluorescence responses of the cantaloupe surfaces, and were not suitable for detection of fecal contamination on cantaloupes due to the presence of false positives. Images constructed using 2-band ratios enhanced the contrast between the fecal-contaminated spots and cantaloupe surfaces. However, ratio images also exhibited false positives emanating from features found on cantaloupes such as scarred tissues. The PCA of hyperspectral images demonstrated the potential detection of feces-contaminated spots (a minimum of 16- μ g/mL dry fecal matter) on cantaloupes with minimal false positives. Examination of PC weighing coefficients defined several dominant

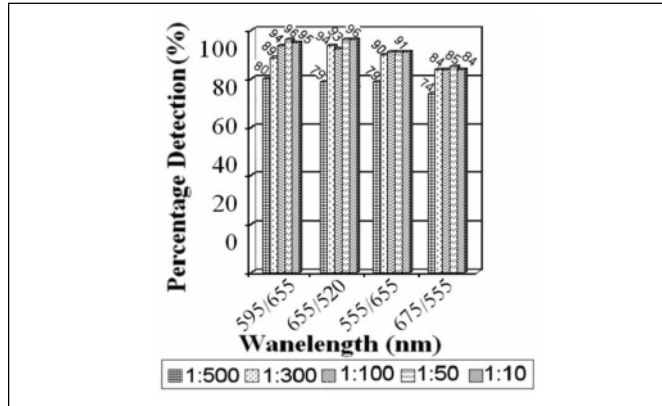


Figure 6—Fecal contamination detection rates for 40- μ L treatment spots for ratio images of 595/655, 655/520, 555/655, and 675/555 nm subjected to the ISODATA (Iterative Self-Organizing Data Analysis Technique) classification method ($n = 80$ per dilution). Note that these ratios represent the 2-band ratio combinations with the highest detection rates.

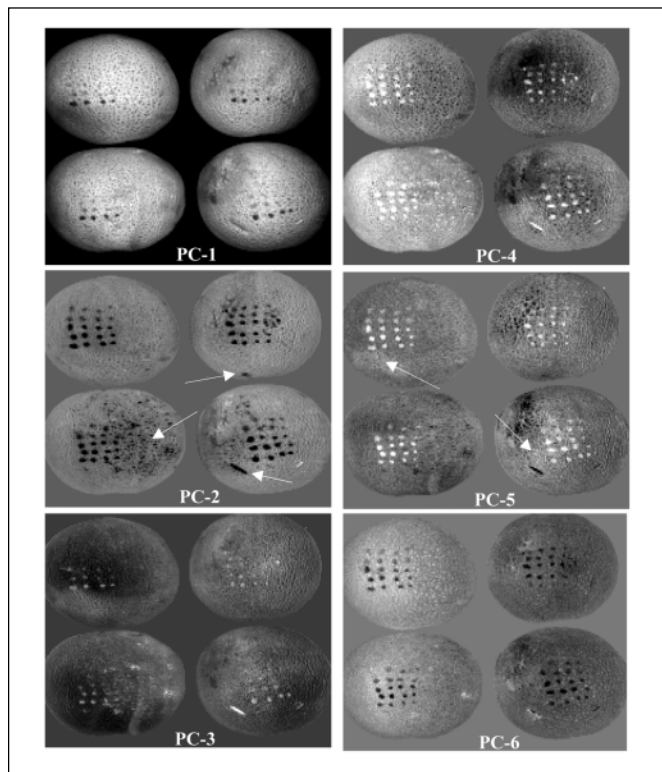


Figure 7—First to 6th principal component (PC) images of bovine feces-treated cantaloupes obtained from principal component analysis (PCA) of the entire hyperspectral fluorescence image data (79 spectral channels). Arrows indicate some of false positives.

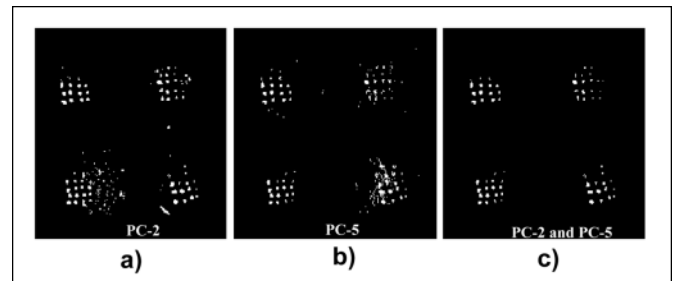


Figure 8—Binary images for feces-contamination spots obtained by subjecting (a) principal component (PC)-2 and (b) PC-5 images to a simple thresholding method (Kim and others 2004). (c) Binary image shows where both PC-2 and PC-5 binary results overlapped. As the resulting binary image illustrates, pixel locations of the PC-2 false positives did not coincide with those of PC-5.

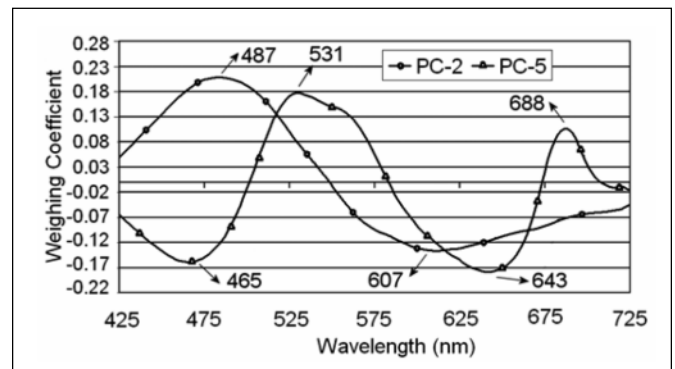


Figure 9—Spectral weighing coefficients (eigenvectors) for principal component (PC)-2 and PC-5. The dominant wavelengths are indicated on the graph.

wavelengths that can be implemented to a multispectral imaging system for online applications.

Acknowledgments

The authors would like to thank the Instrumentation and Sensing Laboratory (ISL), United States Dept. of Agriculture (USDA), the Food and Drug Administration (USFDA), The Joint Inst. of Food Safety and Nutrition (JIFSAN), and the Dept. of Biological Resources Engineering (BRE) at the Univ. of Maryland at College Park (UMCP) for supporting this work. The authors would like to thank Ms. Diane Chan and Mr. John Kelly of ISL for their assistance in sample collection.

References

- Abbott JA, Lu R, Upchurch BL, Strohline RL. 1997. Technologist for non-destructive quality evaluation of fruit and vegetables. *Hortic Rev* 20:1-120.
- Anderson J, Stenzel S, Smith K, Labus B, Rowley P, Shoenfeld S, Gaul L, Ellis A, Fyfe M, Bangura H, Varma J, Painter J. 2002. Multistate outbreaks of *salmonella* serotype poona infections associated with eating cantaloupe from Mexico—United States and Canada, 2000-2002. *Morb Mortal Wkly Rep* 51(46):1044-7.
- Ball GH, Hall DJ. 1965. ISODATA, a novel method of data analysis and pattern classification. Stanford: Stanford Research Inst. Technical Report.
- Chappelle EW, McMurtrey JE, Kim MS. 1991. Identification of the pigment responsible for the blue fluorescence band in laser induced fluorescence spectra of green plants, and the potential use of this band in remotely estimating rates of photosynthesis. *Remote Sens Environ* 36:213-8.
- Chen YR, Chao K, Kim MS. 2002. Machine vision technology for agricultural applications. *Comp Electr Agric* 36:173-91.
- Duda RO, Hart PE, Stork DG. 2001. *Pattern classification*. 2nd ed. New York: Wiley-Interscience. p 114-7.
- Kim MS, Chen YR, Mehl PM. 2001. Hyperspectral reflectance and fluorescence imaging system and safety. *Trans ASAE* 44(3):721-9.
- Kim MS, Lefcourt AM, Chen YR. 2003. Optical fluorescence excitation and emission bands for detection of fecal contamination. *J Food Protect* 66(7):1198-207.
- Kim MS, Lefcourt AM, Chen YR, Kang S. 2004. Hyperspectral and multispectral laser induced techniques for food safety inspection. *Key Eng Mater* 270:1055-63.
- Kim MS, Lefcourt AM, Chen YR, Kim I, Chan DE, Chao K. 2002. Multispectral detection of fecal contamination on apples based on hyperspectral imagery. Part II. Application of hyperspectral fluorescence imaging. *Trans ASAE* 45(6):2039-47.
- Lay D. 2002. *Linear algebra and its applications*. New York: Addison-Wesley. p 441-86.
- Murdock DI, Brokaw CH. 1957. Some specific source of contamination in processing frozen concentrated orange juice. 1. handling and preparing fruit for extraction. *Proc Fla State Hort Soc* 70:231-7.
- Papageorgiou G. 1975. Chlorophyll fluorescence: an intrinsic probe of photosynthesis. In: Govindjee JA and Ford DC. *Bioenergetic of photosynthesis*. 1st ed. New York: Academic Press. p 320-71.
- Pohl C, Van Genderen JL. 1998. Multisensor image fusion in remote sensing: concepts, methods, and application. *J Remote Sens* 19(5):823-54.
- Richards JA. 1986. *Remote sensing digital image analysis: an introduction*. Berlin: Springer-Verlag.
- [USFDA] U.S. Food and Drug Admin. 1998. Guide to minimize microbial food safety hazards for fresh fruit and vegetables. Washington D.C.: Center for Food Safety and Applied Nutrition. Available from: <http://www.cfsan.fda.gov>. Accessed Oct 3, 2005.
- [USFDA] U.S. Food and Drug Admin. 2001. Analysis and evaluation of prevention control measures for the control and reduction/elimination of microbial hazards on fresh and fresh-cut produce. Washington D.C.: Center for Food Safety and Applied Nutrition. Available from: <http://www.cfsan.fda.gov>. Accessed Oct 3, 2005.
- [USFDA] U.S. Food and Drug Admin. 2002. Import alert IA2201: Detection without physical examination of cantaloupes from Mexico. College Park, Md.: Center for Food Safety and Applied Nutrition. Available from: www.fda.gov. Accessed Oct 3, 2005.
- Van Genderen JL, Pohl C. 1994. Image fusion: issues, techniques and applications. Intelligent image fusion. Sept 11, 1994. Proceedings EARSel Workshop; Strasbourg, France. p 18-26.